

# **Mechanical Properties and Microstructure of Biomorphic Silicon Carbide Ceramics Fabricated from Wood Precursors**

M. Singh  
QSS Group, Inc.  
NASA Glenn Research Center  
Cleveland, OH 44135

J.A. Salem  
Structures Division  
NASA Glenn Research Center  
Cleveland, OH 44135

## **Abstract**

Silicon carbide- based, environment friendly, biomorphic ceramics have been fabricated by the pyrolysis and infiltration of natural wood (maple and mahogany) precursors. This technology provides an eco-friendly route to advanced ceramic materials. These biomorphic silicon carbide ceramics have tailorable properties and behave like silicon carbide based materials manufactured by conventional approaches. The elastic moduli and fracture toughness of biomorphic ceramics strongly depend on the properties of starting wood performs and the degree of molten silicon infiltration. Mechanical properties of silicon carbide ceramics fabricated from maple wood precursors indicate the flexural strengths of  $344\pm 58$  MPa at room temperature and  $230\pm 36$  MPa at  $1350^{\circ}\text{C}$ . Room temperature fracture toughness of the maple based material is  $2.6\pm 0.2$  MPa $\sqrt{\text{m}}$  while the mahogany precursor derived ceramics show a fracture toughness of  $2.0\pm 0.2$  MPa $\sqrt{\text{m}}$ . The fracture toughness and the strength increase as the density of final material increases. Fractographic characterization indicates the failure origins to be pores and chipped pockets of silicon.

This report is a preprint of an article submitted to a journal for publication. Because of changes that may be made before formal publication, this preprint is made available with the understanding that it will not be cited or reproduced without the permission of the author.

## 1. Introduction

Silicon-based ceramic materials are either currently being used or are under active consideration for use in a wide variety of applications within the aerospace, nuclear, energy, process, and transportation industries. These materials have high strength, good oxidation and corrosion resistance, high thermal conductivity, and good thermal shock resistance. A number of manufacturing approaches have been used to fabricate these materials including hot pressing/hot isostatic pressing, sintering, reaction bonding/reaction forming, polymer pyrolysis, and chemical vapor deposition. Hot pressing and sintering approaches require significant consumption of energy while CVD and polymer pyrolysis techniques generate liquid and gaseous chemical by-products that have to be scrubbed and treated. The reaction bonding technique typically utilizes silicon carbide and carbon powder combined with polymer binders while reaction forming techniques require porous preforms derived from resin. As with hot pressing and sintering, the production of silicon carbide powder is energy intensive. The pyrolysis of resin systems produces chemical by-products, which have to be collected for disposal.

Due to the aforementioned environmental and economical issues associated with traditional manufacturing, there recently has been a great deal of interest in utilizing biomimetic approaches to fabricate a wide variety of silicon-based ceramic materials. A number of these fabrication approaches have utilized natural wood or cellulosic fibers to produce carbon preforms. Wood is a “lignocellulosic” material formed by the photosynthetic reaction within the needles or leaves of trees. The photosynthesis process uses sunlight to take carbon dioxide from air and convert it into oxygen and organic materials. The result, wood, has been one of the best and most intricate engineering materials created by nature and known to mankind [1-2]. In addition, natural woods of various types are available throughout the world. Even the sawdust generated in abundant quantities by sawmills is useful. Eco-ceramic materials, fabricated via the pyrolysis and reactive infiltration with various liquid and gaseous reactants into natural wood-derived

preforms, have tailorable properties with numerous potential applications. The experimental studies conducted to date on the development of ceramics based on biologically derived structures, indicate that these materials behave like conventional manufactured ceramics [3-15]. In addition, these structures have been shown to be quite useful in producing porous or dense ceramics having various microstructures and compositions.

In this study, natural mahogany and maple wood has been used to fabricate SiC ceramics through a process of pyrolysis and liquid silicon infiltration as described in previous publications [5-15]. The natural internal channels of wood allow the silicon infiltration, and result in a network of SiC after the reaction with carbon. In this report, the pyrolysis process, microstructure, and mechanical properties (elastic modulus, fracture toughness, and flexural strength) of SiC ceramics fabricated from mahogany and maple wood is presented in detail.

## **2. Experimental Procedures**

Thermal characterization of the pyrolysis process was performed using thermogravimetry (TG) and differential scanning calorimetry (DSC). These two techniques were used simultaneously to measure the change in sample mass with temperature as well as changes in enthalpy that occur during pyrolysis. The Netzsch Thermische Analyser STA 409C was used in this process, with alumina powder as the reference sample.

Rectangular test specimens (20 cm long x 5 cm wide x 3 cm thick) were cut from large blocks of maple and mahogany wood. These wood pieces were dried in an oven at 100°C for four hours and pyrolyzed in a furnace up to 1000°C in a flowing argon atmosphere to create carbonaceous preforms. The weight and dimensional changes were recorded after pyrolysis. The pyrolyzed preforms were infiltrated with silicon in a graphite element furnace under vacuum. Generally, the infiltration time and temperature depend on the

melting point of the infiltrants and dimensions and properties of the preforms. For silicon, infiltration at 1450°C for 30 minutes is adequate. After the infiltration, specimens were machined for microstructural and mechanical property studies. Samples were cross-sectioned and polished for metallographic studies. Microstructural characterization was performed on the as-fabricated and tested samples using optical and scanning electron microscopy. The final product has a cellular structure with areas of SiC and Si.

After the melt infiltration, flexure bars were machined from the infiltrated plates. Four-point flexural strength testing was carried out using ASTM C 1161 configuration B specimens with 20 mm inner and 40 mm outer spans. Flexure tests were conducted at room temperature, 800, 1200, 1300, and 1360°C in air. Three to five specimens were tested at each temperature. The fracture toughness was measured by using the chevron-notch flexure test method as described in ASTM C 1421. At least three specimens were used for the fracture toughness and elastic modulus measurements. After testing, fracture surfaces were examined by optical and scanning electron microscopy to identify the failure origins.

### **3. Results and Discussion**

#### ***3.1 TGA/DSC Analysis***

In order to study the decomposition behavior of these two woods, small pieces were heated in the thermal analyzer up to 1000°C in the inert atmosphere. The wood pyrolysis process typically starts around 200°C and the majority of decomposition is completed around 500°C, depending on the type of wood. Wood consists of three major macromolecular constituents, namely cellulose, hemicellulose, and lignin. Typically, half of the dry weight of wood is cellulose, and hemicellulose and lignin consists of other half (~25% each). The exact amount of these constituents changes with the specific nature and

type of wood. The overall pyrolysis process of wood has been studied by a number of investigators and summarized in a recent review publication [16].

Fig. 1 (a) and (b) shows the thermogravimetric analysis (TGA) and differential scanning calorimetry (DSC) curves of maple and mahogany wood up to 1000°C. There are similarities in the decomposition process. During the initial heating of the specimens, the removal of moisture starts around 100°C and is completed around 170°C. During the second step of weight loss, the decomposition of hemicellulose takes place at around 190-280°C and volatile products are released (CO<sub>2</sub>, CO, and other organics vapors). In the temperature range of 280-500°C, major weight loss takes place due to the decomposition of cellulose and lignin. The decomposition of lignin increases above 300°C and results in a rapid increase in carbon content of the material [16]. Typically, the majority of the decomposition is completed by 500°C, and minimal weight loss occurs afterwards. The major weight loss events are shown in DSC curves, which exhibit the endothermic and exothermic nature of the reactions. Although the TGA curves for both woods are quite similar in their nature, the DSC curves show slight differences due to differences in the chemical contents of maple and mahogany woods.

### **3.2 Microstructure**

A number of maple and mahogany specimens were pyrolyzed and infiltrated in this study. The starting density of the dried wood (~0.64-0.66 gm/cm<sup>3</sup>) and the density of pyrolyzed preforms (0.50-0.52 gm/cm<sup>3</sup>) from both woods were quite similar. Scanning electron micrographs of fracture surfaces of maple wood-derived porous carbon preforms are shown in Figs. 2 (a)-(b). This microstructure shows a heterogeneous pore size distribution (large and small pores). Optical micrographs of the liquid silicon infiltrated maple are shown in Figs. 2 (c) and (d). The gray areas in the micrographs are silicon carbide and the white areas are residual silicon. During the reactive infiltration processing, silicon infiltrates through the pores and channels of the pyrolyzed wood

structure and reacts with the carbon. Some of the large pores (black area in the micrographs) have not been completely filled with silicon. The final material was not completely dense and there was density variation in the infiltrated plates and subsequently in the machined flexural bars. The densities of the individual bars varied from 2.16-2.72 gm/cm<sup>3</sup> with an average of about 2.36 gm/cm<sup>3</sup>. The density of silicon carbide and silicon are 3.21 and 2.33 gm/cm<sup>3</sup>, respectively.

The microstructure of the porous carbon performs from mahogany wood precursors are shown in Figs. 3 (a-d) in two different directions respective to tree growth. As with the maple-based material, the mahogany exhibits a heterogeneous pore size distribution (large and small pores). Microstructures of the silicon carbide based materials obtained after silicon infiltration are shown in Figs. 4 (a) and (b). In these micrographs, silicon carbide regions are gray and silicon regions are white. This material also contains porosity (black regions). The density of individual bars of silicon carbide from mahogany varied from 1.97-2.04 gm/cm<sup>3</sup> with an average of about 2.00 gm/cm<sup>3</sup>.

These micrographs show variation in the microstructure and density of the carbonaceous performs, due to the structural differences within a wood sample and between various types of wood. The variation of preform microstructure and properties can be utilized to produce final materials with controlled composition and phase morphologies. The pyrolysis shrinkage, composition, and final density of preforms vary greatly depending on the type of wood. The perform density and microstructure control the composition and microstructure of final materials. Microstructure and mechanical properties of a wide variety of wood specimens have been investigated and reported in other publications [9-15].

### ***Elastic Modulus***

The elastic moduli of some of the flexural specimens were measured by using the impulse excitation technique [17]. The length of the flexural specimens was parallel to the growth

direction of wood. Test specimens were supported at the nodal points with foam strips and the specimen impacted lightly. The resultant impact induced flexural vibration that was detected with a piezoelectric crystal and automatically recorded with an electronic circuit. The elastic moduli were then calculated from the specimen geometry and measured resonant frequency. The elastic moduli of the maple and mahogany based materials were  $250 \pm 23$  and  $178 \pm 18$  GPa respectively along the growth direction. The elastic moduli of sintered silicon carbide (Hexoloy-SA) is 420 GPa and reaction bonded silicon carbide (Norton NC 435) is 340 GPa [18]. The amount of silicon and porosity plays a critical role in the elastic moduli of these materials. The large standard deviations were a result of billet-to-billet density variations. The bulk density of the maple and mahogany based materials were typically  $2.27 \pm 0.07$  and  $2.00 \pm 0.3$  g/cm<sup>3</sup>, respectively.

### ***Flexural Strength***

Strength testing was conducted by using four-point flexure with 20 mm load and 40 mm support spans [19] at room temperature, 800°C, 1200, and 1350°C. Three tests were conducted per temperature, and a stroke rate of 0.5 mm/min was used. The room and high temperature flexural strengths of the as-machined materials are shown in Fig. 5. The maple base material exhibited a substantially higher strength at all temperatures, with mean strengths of  $344 \pm 58$ ,  $275 \pm 33$ ,  $283 \pm 29$ , and  $230 \pm 36$  MPa at room, 800, 1200, and 1350°C, respectively. The mahogany based material exhibited strengths of  $144 \pm 13$ ,  $128 \pm 30$ ,  $118 \pm 10$ , and  $112 \pm 11$  MPa at room, 800, 1200, and 1350°C, respectively. The flexure strength is compared to that of a commercially available reaction bonded silicon carbide material (Cerastar RB-SiC) in figure 5. The flexural strength data shows that there is relatively little strength loss for these materials at temperatures up to 1200°C, and the strength is comparable to that of a commercial RB-SiC material. Considering that the melting point of silicon is  $\sim 1410^\circ\text{C}$ , the constant strength of both materials between

room temperature and 1300°C, is surprising. This is likely a result of the strength being controlled by the stiff network of SiC formed from the carbon perform.

SEM fractographs of the tested mahogany flexure specimens are shown in Figs. 6 (a)-(b). Although the porosity in these materials was believed to act as the failure origins, the specific origins could not be identified due to the coarse structure and the low failure strength. Some of these pores were also filled with silicon (Fig. 6 b).

Figure 7 and 8 show failure origins in the <sup>SiC</sup> Maple material. In one specimen, failure initiated from the edge of a ~110 μm silicon pocket that contained a ~50 μm pore. In other cases, failure initiated from a pocket of silicon that was connected to the surface and likely chipped during machining. Large pocket<sup>s</sup> of silicon are likely to be detrimental to the material in several ways: The fracture toughness of silicon is approximately 1 MPa√m, and thus large flaws in silicon pockets causes the fracture toughness to effectively drop. Further, pockets of silicon are more likely to be chipped during machining than the surrounding SiC.

### ***Fracture Toughness***

Two of the test methods standardized by ASTM [20] were applied in an attempt to measure the fracture toughness of these materials: the SEPB (Single-Edged-Pre-cracked-Beam) and the CN (chevron-notch) methods. Neither method initially yielded valid results. In the case of the SEPB, the Vickers's indentations that are used to start the through-section pre-crack did not emanate starter-cracks from the indentation corners. This was likely due to the porosity of the material. As a result, a through-section pre-crack for fracture toughness measurement could not be generated without failing the test specimen. For the CN, stable crack extension, which is required for a valid result, was not obtained. In order to promote stable extension, three-point flexure was used rather than 4-point flexure, and the stress intensity factor coefficient appropriate modified. Although

this did not completely stabilize the specimen, it did result in a series of small crack-jumps through maximum load, thereby allowing a good estimate of the fracture toughness. To validate the modified, three-point test method, a test was run on a batch of well-characterized alpha silicon carbide. The three-point result and valid results generated previously by using ASTM C1421 were in excellent agreement ( $2.60 \text{ MPa}\sqrt{\text{m}}$  vs.  $2.61 \pm 0.05 \text{ MPa}\sqrt{\text{m}}$ ).

The fracture toughness,  $K_{Ivb} (A)$  of the maple based ecoceramic was  $2.6 \pm 0.2 \text{ MPa}\sqrt{\text{m}}$ , which is comparable to that of alpha silicon carbide as measured with the same technique ( $2.61 \text{ MPa}\sqrt{\text{m}}$  [21]). The fracture toughness of the mahogany based ecoceramic was significantly lower at  $2.0 \pm 0.2 \text{ MPa}\sqrt{\text{m}}$ .

Although C 1421 [20] contains a third test method (the surface crack in flexure), the lack of starter-crack formation at indentation sites implied that the technique would not work, and it was not pursued.

### ***Correlation of Mechanical Properties to Density***

A good correlation between room temperature elastic modulus (measured using Grindosonic technique) and bulk density was apparent on a specimen-by-specimen basis for both materials, as shown in Fig. 9. However, there was no clear correlation in the high temperature flexure strength and the elastic modulus measured using the test specimen compliance during the high temperature flexure tests. This data for both sets of specimens as a function of temperature is shown in Fig. 10. The strength for maple-based material is likely controlled by local features/variations in the microstructure rather than slight variation in the density.

Correlation between fracture toughness and density could not be clearly established on a specimen-by-specimen basis; however, the fracture toughness and density of the maple are greater than that of the mahogany, as shown in Fig. 11. This is not too surprising because fracture toughness as measured with the chevron-notch sample much of the cross section. If the material has a lower density, then less material is available to resist extension of the crack, whereas if the material is dense, more new surface area must be created.

#### **4. Conclusions**

Biomorphic SiC-based ceramics have been fabricated from renewable, natural resources. These ceramic materials have a consistent microstructure that resembles the microstructure of the wood preform. They behave as a silicon carbide-based cellular solid, reaching very high strengths. For a maple-based ceramic, fracture toughness and strength approach that of silicon carbide fabricated via conventional routes was obtained. The low cost, flexibility to fabricate complex shapes, and the availability of unique microstructures in nature makes this fabrication technique very promising for producing materials suitable for structural and lightweight applications.

#### **5. Acknowledgements**

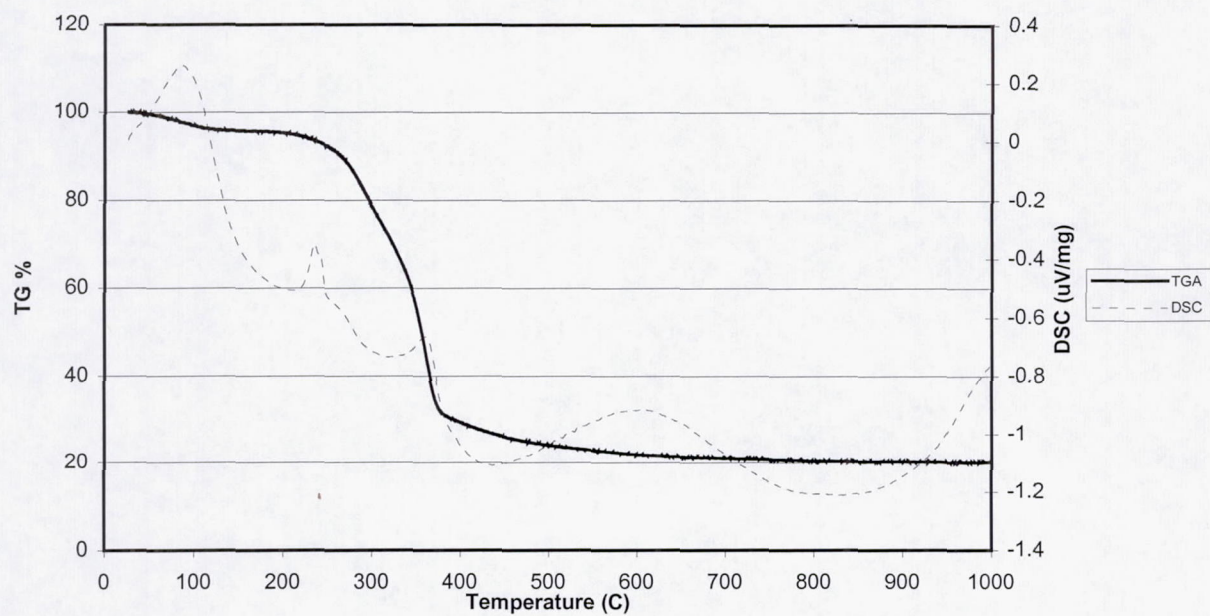
The author would like to thank Mr. Richard Dacek and Mr. Ron Philips for help in experimental work.

#### **References**

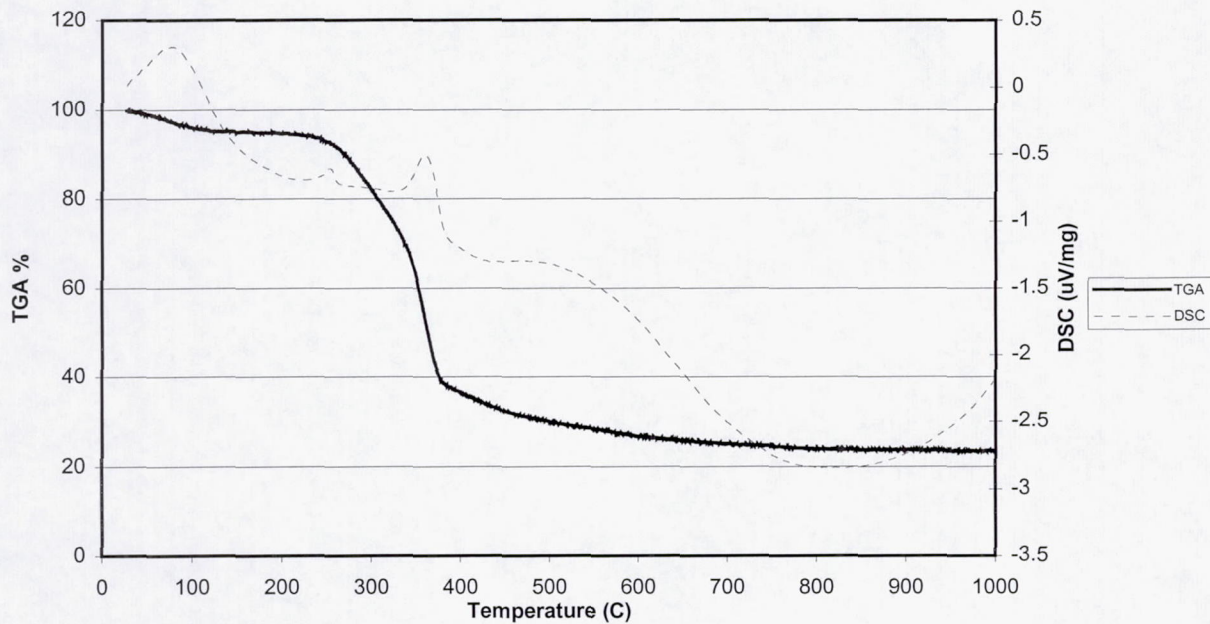
- [1] *Wood Handbook- Wood as an Engineering Material*, Forest Products Laboratory, USDA Forest Service, Madison, WI, General Technical Report, FPL-GTR-113, 1999.
- [2] *Concise Encyclopedia of Wood and Wood-Based Materials*, A.P. Scniewind, Ed., Pergamon Press, NY, 1989.

- [3] Mark, J.E. and Calvert, P.D., Biomimetic, hybrid and in-situ composites, *Mater. Sci. and Engg.*, 1994, C1, 159.
- [4] Ota, T., Takahashi, M., Hibi, T., Ozawa, M. and Suzuki, H., Biomimetic process for producing SiC wood, *J. Am. Ceram. Soc.*, 1995, **78**, 3409-3411.
- [5] Greil, P., Lifka, T. and Kaindl, A., Biomorphic silicon carbide ceramics from wood: I and II, *J. Eur. Ceram. Soc.*, 1998, **18**, 1961-1983.
- [6] Griel, P., Biomorphic ceramics from lignocellulosics, *J. Eur. Ceram. Soc.*, 2001, 21 105-118.
- [7] Shin, D.-W., Park, S.S., Choa, Y.-H., and Niihara, K., Silicon/silicon carbide composites Fabricated by infiltration of a silicon melt into charcoal, *J. Am. Ceram. Soc.*, 1999, **82**, 3251-54.
- [8] Nagle, D.C. and Bryne, C.R., Carbonized wood and materials formed there from, US Patent 6, 124, 028, 2000.
- [9] Singh, M., Environment conscious ceramics (Ecoceramics), *Ceram. Sci. Engg. Proc.*, 2000, 21 (4) 39-44.
- [10] Martínez-Fernández, J., Valera-Feria, F.M. and Singh, M., High temperature compressive mechanical behavior of biomorphic silicon carbide ceramics, *Scripta Materialia*, 2000, 43, 813-818.
- [11] Martínez-Fernández, J., Valera-Feria, F.M., Domínguez Rodríguez, A. and Singh, M., Microstructure and Thermomechanical characterization of biomorphic silicon carbide-based ceramics, pp. 733-740 in *Environment Conscious Materials; Ecomaterials*. Edited by H. Mostaghaci, Canadian Institute of Mining, Metallurgy, and Petroleum. Quebec, Canada, 2000.
- [12] Qiao, G., Ma, R., Cai, N., Zhang, C. and Jin, Z., Mechanical properties and microstructure of Si/SiC materials derived from native wood, *Mater. Sci. Engg.*, 2002, A 323, 301-305.
- [13] Singh, M., Environment conscious ceramics (Ecoceramics)", NASA/TM-2001-210605, NASA Glenn Research Center, Cleveland, OH, 2001.
- [14] Singh, M., Ecoceramics: ceramics from wood, *Advanced Materials and Processes*, 2002, 160 (3), 39-41.

- [15] Singh, M. and Yee, Bo-Moon, Environment conscious, biomorphic silicon carbide based ceramics from pine and jelutong precursors, *Ceramic Engineering and Science Proceedings*, The American Ceramic Society (2002) in press.
- [16] Sinha, S., Jhalani, A., Ravi, M.R., and Ray, A., Modeling of pyrolysis in wood: a review, *J. Solar Energy Society of India*, 2000, 10 (1) 41-62.
- [17] ASTM C 1259-98, Standard Test Method for Dynamic Young's Modulus, Shear Modulus, and Poisson's Ratio for Advanced Ceramics by Impulse Excitation of Vibration, in *Annual Book of ASTM Standards*, American Society for Testing and Materials, West Conshohocken, Pennsylvania, 1999, Vol. 15.01, 386-400.
- [18] Singh, M., Pawlik, R., Salem, J.A., and D.R. Behrendt, Mechanical properties of reaction-formed silicon carbide ceramics containing silicon and refractory disilicide phases, in *Advances in Ceramic Matrix Composites*, The American Ceramic Society, Westerville, Ohio 1993, 349-360.
- [19] ASTM C 1161-94, Standard Test Method for Flexural Strength of Advanced Ceramics at Ambient Temperature, in *Annual Book of ASTM Standards*, American Society for Testing and Materials, West Conshohocken, Pennsylvania, 1999, Vol. 15.01, 309-315.
- [20] ASTM C 1421-99, Standard Test Method for the Determination of Fracture Toughness of Advanced Ceramics at Ambient Temperatures, in *Annual Book of ASTM Standards*, American Society for Testing and Materials, West Conshohocken, Pennsylvania, 2000, V 15.01, 631-662.
- [21] Salem, J.A., Ghosn, L., Jenkins, M.G. and Quinn, G.D., Stress Intensity Factor Coefficients for Chevron-notched Flexure Specimens and a Comparison of Fracture Toughness Methods, *Ceramic Engineering and Science Proceedings*, 1999, 20 (3), 503-512.

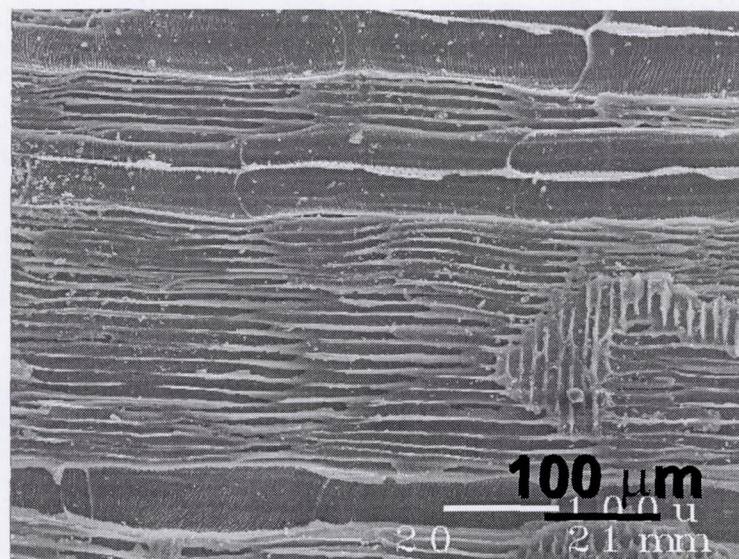


(a)

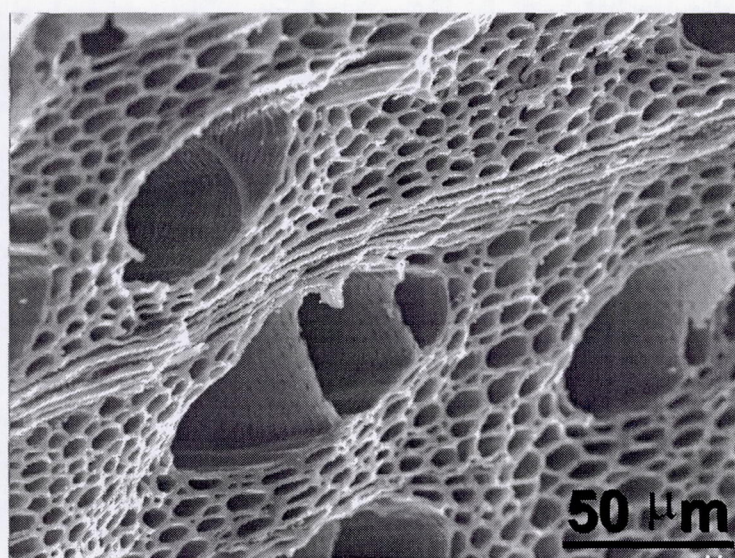


(b)

Fig. 1: DSC and TGA curves for (a) maple and (b) mahogany during the pyrolysis.

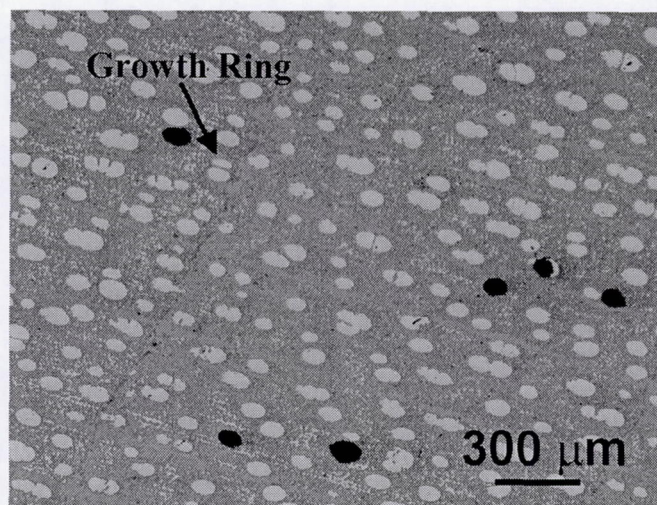


(a)

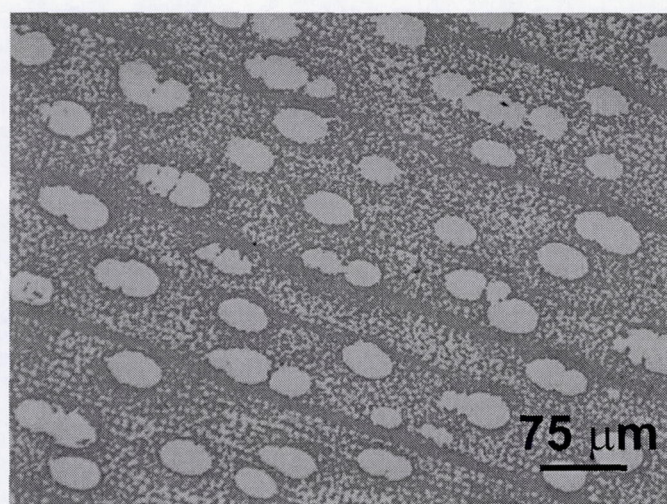


(b)

Fig 2: Scanning Electron Micrographs showing the microstructure of maple derived carbonaceous performs (a) parallel and (b) perpendicular to growth direction.



c



d

Figs 2 (c-d): Optical micrographs showing the microstructure of silicon carbide made from maple. View is perpendicular to the growth direction.

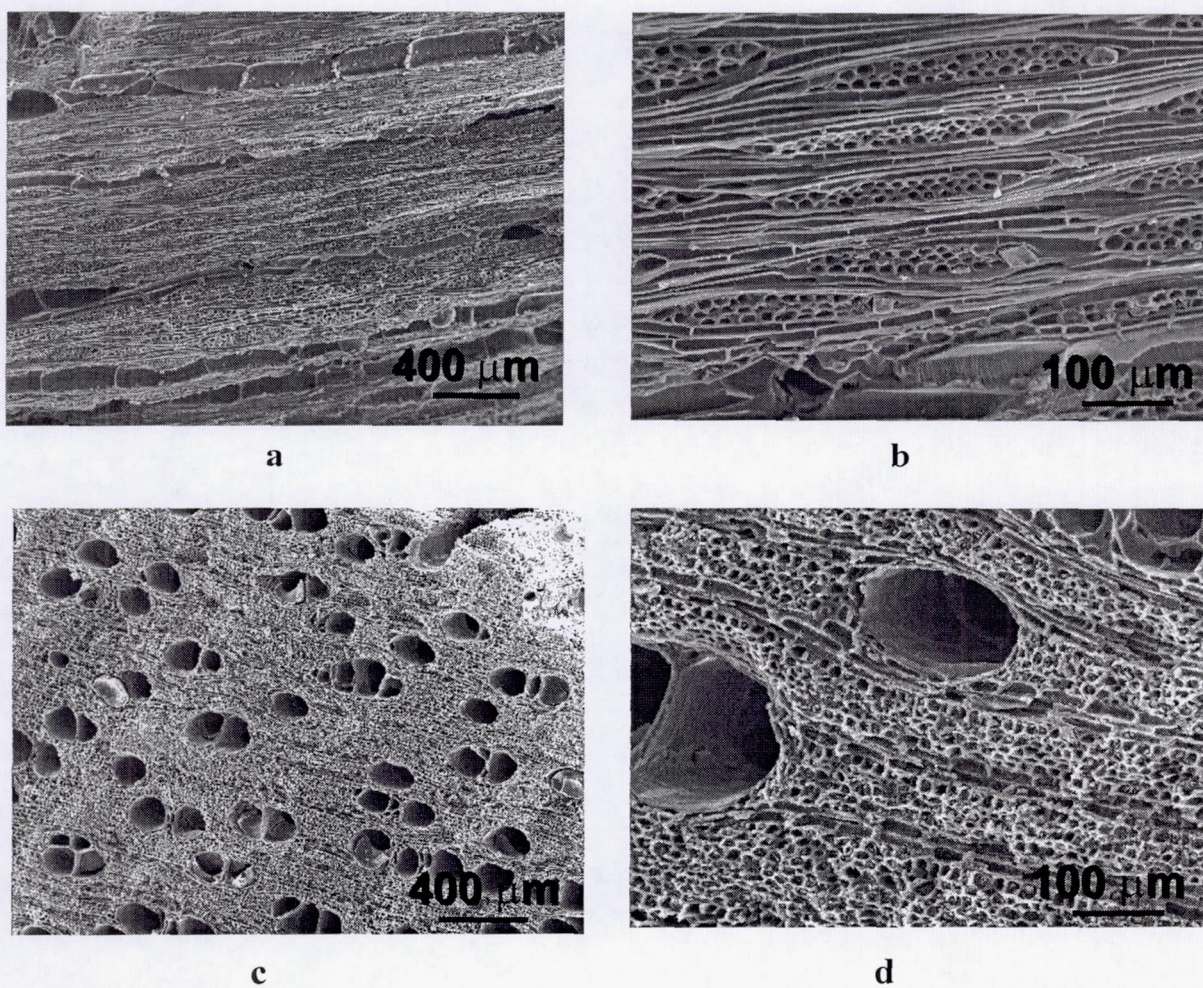
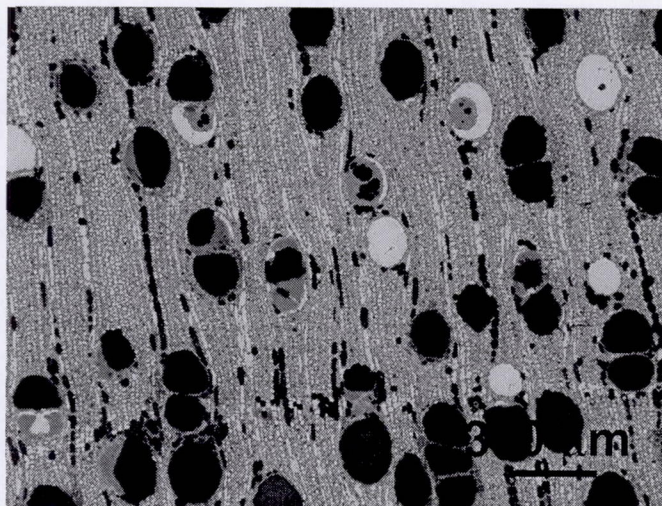
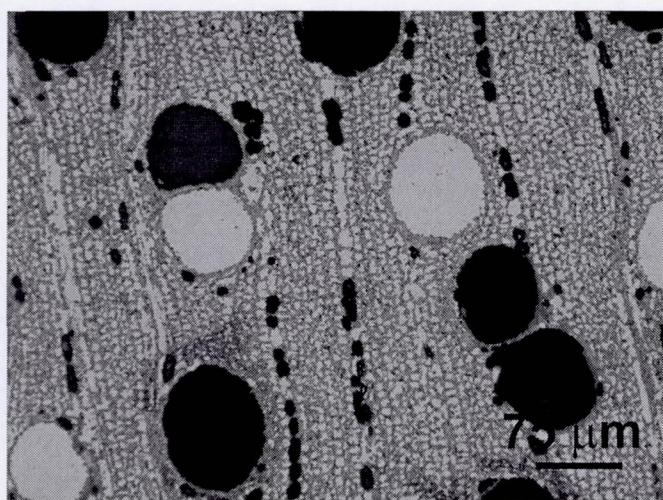


Fig. 3: SEM micrographs of porous carbon performs made from mahogany: (a, b) parallel to the growth direction, and (c, d) perpendicular to growth direction.



a



b

Fig. 4: Optical micrograph of as-fabricated SiC made from mahogany. View is perpendicular to the growth direction (white: Si, gray: SiC, black: pores).

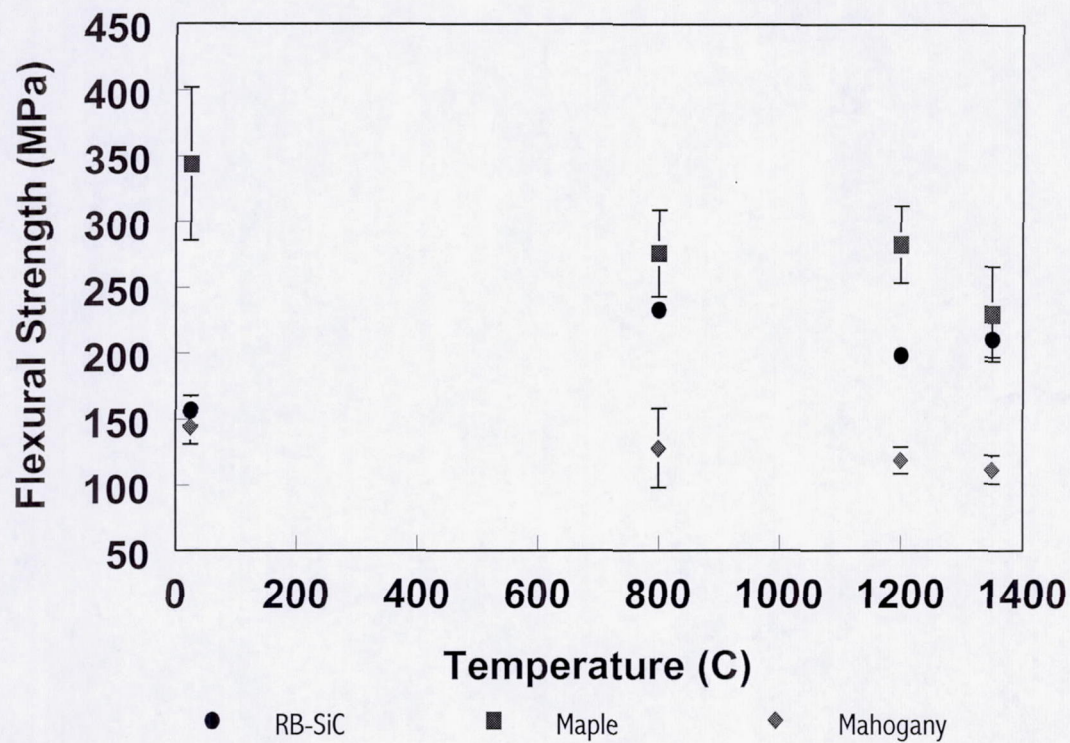
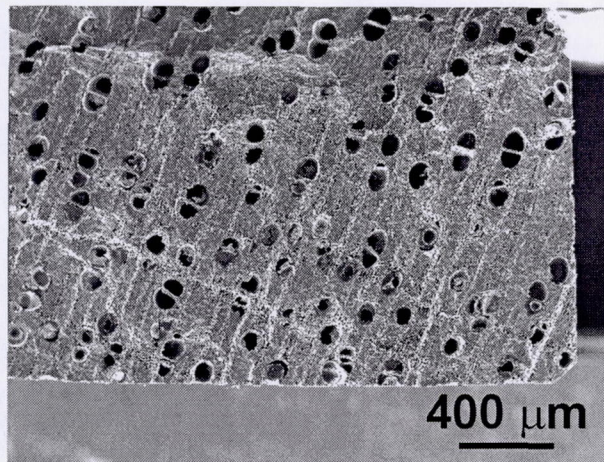
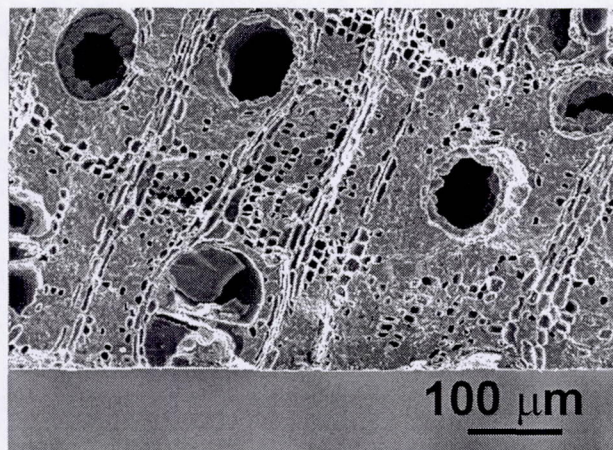


Fig. 5: Flexural strength  $\pm$  one standard deviation as a function of temperature for silicon carbide based ceramics made from Maple and Mahogany. The flexural strength data for CRYSTAR reaction bonded silicon carbide is also shown for comparison.

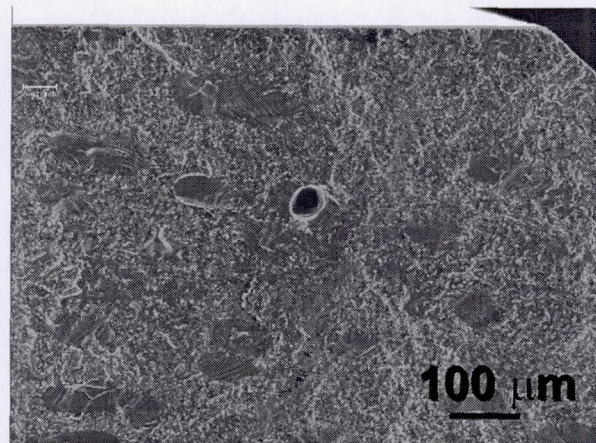


a

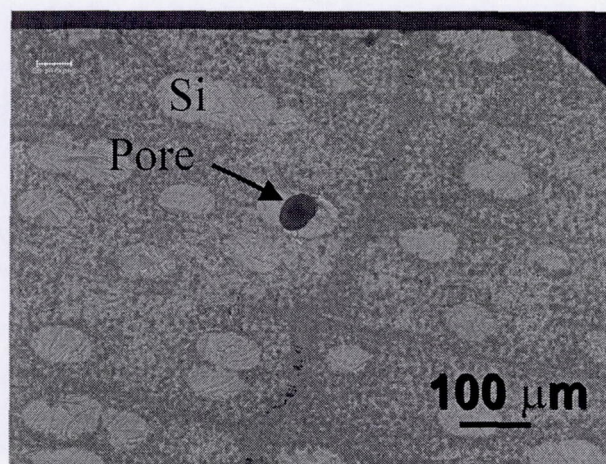


b

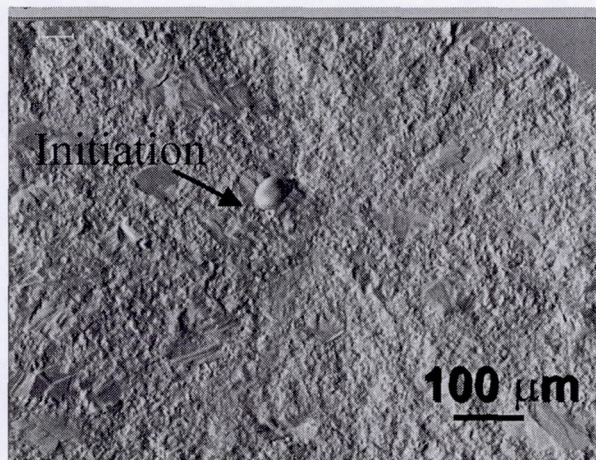
Fig. 6: SEM micrographs showing the fracture surfaces of mahogany-based specimens tested at room temperature.



a



b



c

Fig. 7: SEM fractographs showing the failure origin in maple-based test specimens. Failure occurred from the interface between silicon pockets and silicon carbide phase [(a) SE image, (b) BSE, and (c) topographic image].

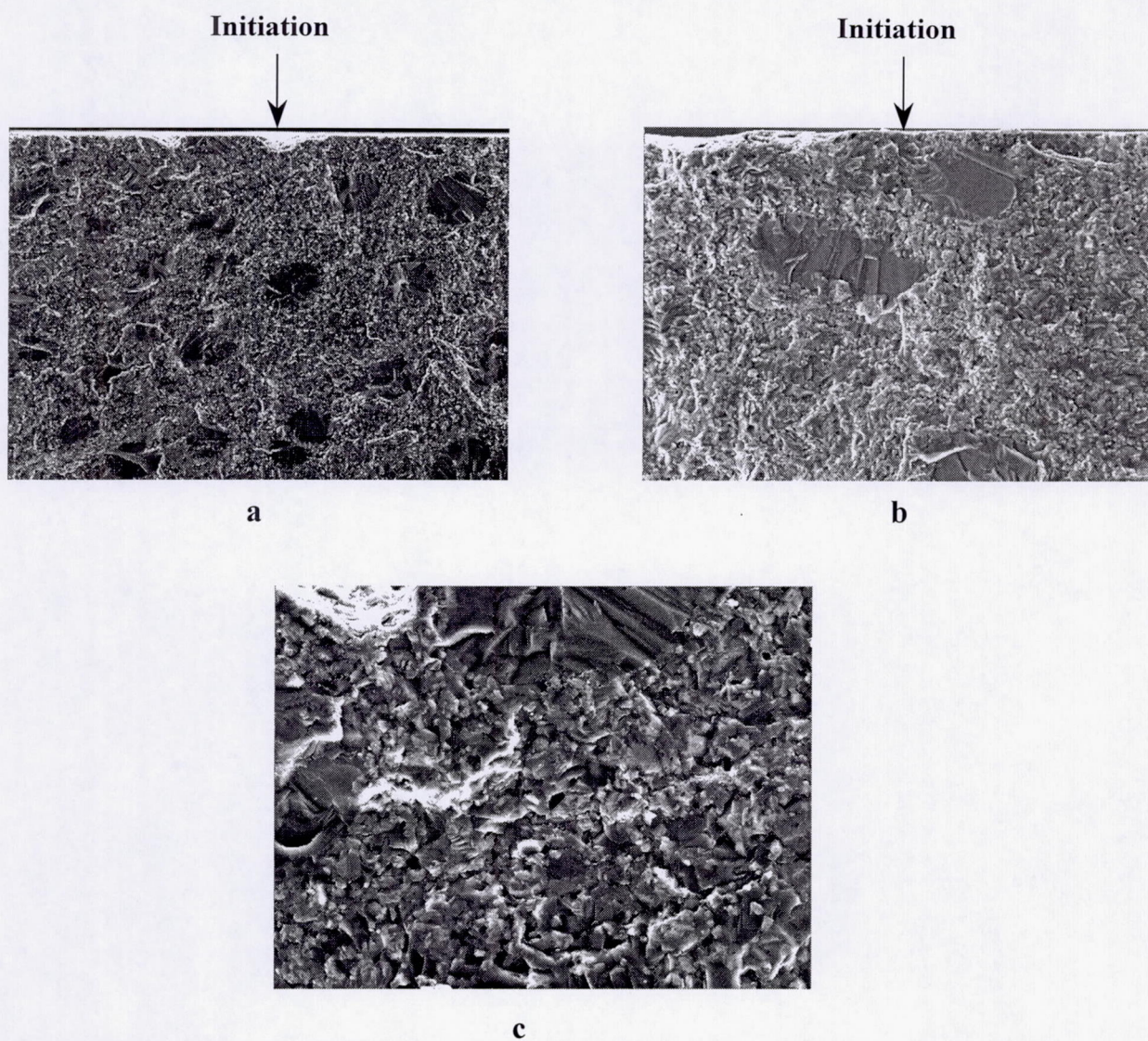


Fig. 8: SEM micrographs showing the fracture surfaces of maple-based specimens tested at room temperature: (a) Chip, (b) region of coarse SiC adjoining a Si pocket (c) chip adjoining a Si pocket.

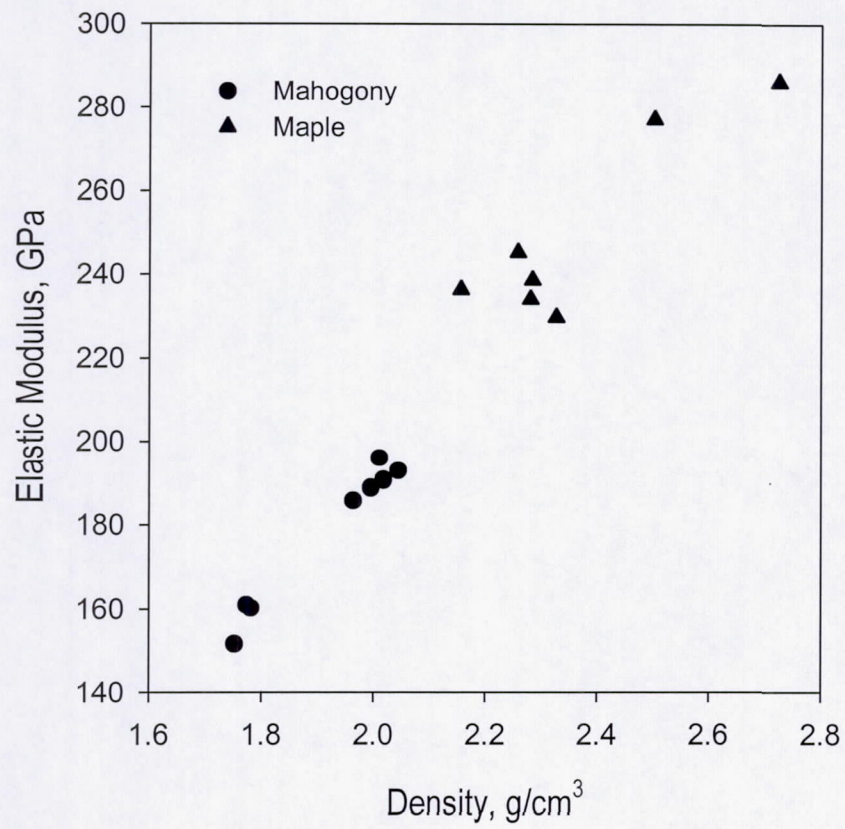


Fig. 9: Elastic Modulus as a function of density for maple and mahogany based eco-ceramics.

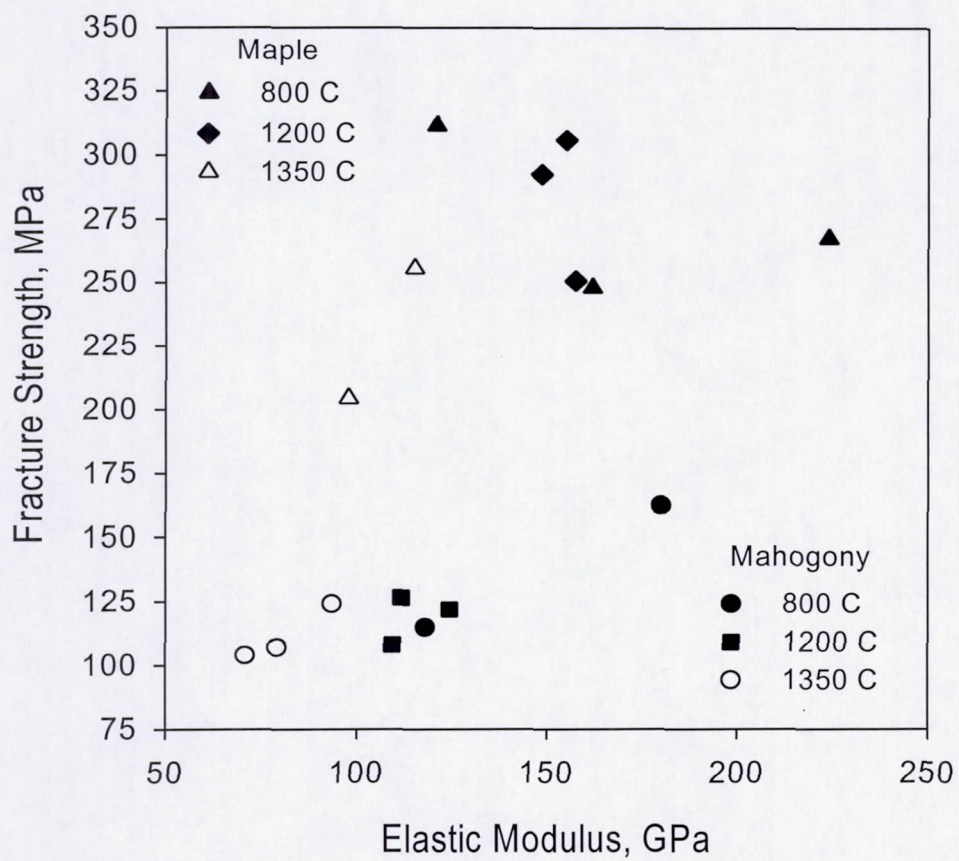


Fig. 10: High temperature fracture Strength as a function of elastic modulus (measured with test specimen compliance) for maple and mahogany based materials.

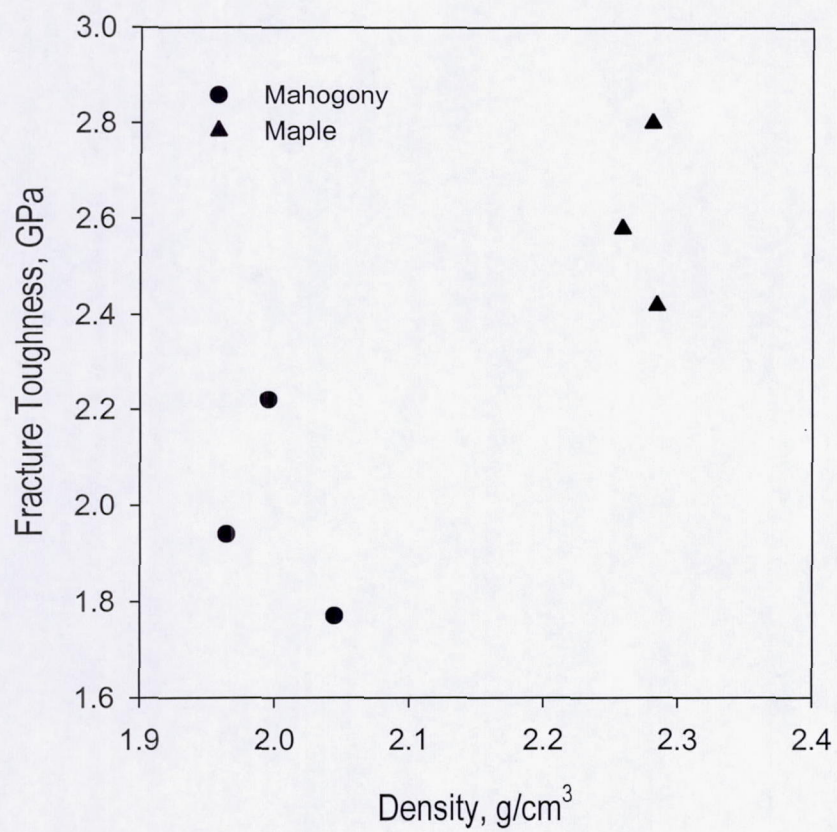


Fig. 11: Fracture Toughness as a function of density for maple and mahogany based eco-ceramics.